NLRP3 leucine-rich repeats control induced and spontaneous inflammasome activation in cryopyrin-associated periodic syndrome

Katerina Theodoropoulou, MD, PhD,[a,b] Lotte Spel, PhD,[a] Léa Zaffalon, MSc,[a] Maeva Delacrétaz, AS,[a] Michaël Hofer, MD,[b] and Fabio Martinon, PhD[a] *Lausanne, Switzerland*

Background: The cryopyrin-associated periodic syndromes (CAPS) comprise a group of rare autoinflammatory diseases caused by gain-of-function mutations in the *NLRP3* gene. NLRP3 contains a leucine-rich repeats (LRR) domain with a highly conserved exonic organization that is subjected to extensive alternative splicing. Aberrant NLRP3 inflammasome assembly in CAPS causes chronic inflammation; however, the mechanisms regulating inflammasome function remain unclear.
Objective: We aimed to elucidate the mechanisms regulating NLRP3-mediated autoinflammation in human disease, characterizing the role of LRR in inflammasome activation.
Methods: We analyzed sequence read archive data to characterize the pattern of NLRP3 splicing in human monocytes and investigated the role of each LRR-coding exon in inflammasome regulation in genetically modified U937 cells representing CAPS and healthy conditions.
Results: We detected a range of NLRP3 splice variants in human primary cells and monocytic cell lines, including 2 yet-undescribed splice variants. We observe that lipopolysaccharides affect the abundance of certain splice variants, suggesting that they may regulate NLRP3 activation by affecting alternative splicing. We showed that exons 4, 5, 7, and 9 are essential for inflammasome function, both in the context of wild-type NLRP3 activation by the agonist molecule nigericin and in a model of CAPS-mediated NLRP3 inflammasome assembly. Moreover, the SGT1-NLRP3 interaction is decreased in nonfunctional variants, suggesting that alternative splicing may regulate the recruitment of proteins that facilitate inflammasome assembly.
Conclusion: These findings demonstrate the contribution of the LRR domain in inflammasome function and suggest that navigating LRR exon usage within NLRP3 is sufficient to dampen inflammasome assembly in CAPS. (J Allergy Clin Immunol 2023;151:222-32.)

Key words: *Inflammasome,* NLRP3*, LRR, cryopyrin, autoinflammatory disease, CAPS, cryopyrinopathies, alternative splicing*

Inflammation is an essential and tightly controlled process initiated by the innate immune system in response to infection and tissue damage. Cytoplasmic multiprotein complexes called inflammasomes are central platforms of innate immunity, promoting the maturation and release of proinflammatory cytokines.[1-3] These complexes are composed of a sensor molecule such as a nucleotide-binding and oligomerization domain–like receptor (NLR), the adaptor protein apoptosis-associated speck-like protein containing a caspase recruitment domain (ASC), and the effector protein caspase-1. Upon assembly, inflammasomes activate caspase-1, which promotes the maturation of proinflammatory cytokines IL-1β and IL-18. Active inflammasomes also cleave gasdermin D (GSDMD) to generate an *N*-terminal fragment that disrupts membranes by forming pores, thereby promoting cytokine release and pyroptosis.[4,5] NLRP3 is an extensively studied inflammasome sensor that belongs to the family of nucleotide-binding oligomerization domain and leucine-rich repeats (LRR)-containing proteins (NLRs). Canonical activation of NLRP3 inflammasome requires 2 signals. Signal 1, also known as priming, licenses inflammasome components for activation and promotes the transcriptional upregulation of inflammasome components and substrates. Signal 2 mediates inflammasome components assembly and promotes its enzymatic activity.[6,7]

NLRP3 is composed of an *N*-terminal Pyrin domain, a central adenosine triphosphatase domain known as NACHT, and a C-terminal LRR domain.[3] The structural unit of one LRR is composed of a β strand and an α helix. The β strands as well as the α helices of multiple LRR align on opposing sides of the molecule, forming a nonglobular, horseshoe-shaped molecule, with the β strands and α helices lining its inner and outer circumference, respectively.[8] The LRR region of NLRP3 is encoded by 6 exons; each except the last has the exact same length of 171 nt and is coding for one half, one entire, and another half LRR. Moreover, the exon–exon junction and the reading frame are conserved among all NLRs in all vertebrates, from zebrafish to humans.[9,10] The reason for this unusually conserved modular organization is unknown, but it allows for extensive alternative splicing (AS) without disturbing the 3-dimensional fold of the protein.

AS is a process during gene expression that allows messenger RNA (mRNA) to direct the synthesis of various protein isoforms that may have distinct properties.[11] During AS, the pattern of

From [a]the Department of Immunobiology, University of Lausanne, and [b]the Pediatric Unit of Immunology, Allergology and Rheumatology, University Hospital of Lausanne, Lausanne.

This work was supported by grants from the Swiss National Science Foundation (F.M.; 310030_173152) and the Institute of Rheumatology Research. L.S. was supported by research program ZonMW with project 452183005, partly financed by the Dutch Research Council (NWO).

Disclosure of potential conflict of interest: The authors declare that they have no relevant conflicts of interest.

Received for publication March 15, 2022; revised July 15, 2022; accepted for publication August 11, 2022.

Available online September 6, 2022.

Corresponding author: Fabio Martinon, PhD, Department of Immunobiology, University of Lausanne, 155 Ch des Boveresses, Epalinges 1066, Switzerland E-mail: Fabio.Martinon@unil.ch.

The CrossMark symbol notifies online readers when updates have been made to the article such as errata or minor corrections

0091-6749

© 2022 The Authors. Published by Elsevier Inc. on behalf of the American Academy of Allergy, Asthma & Immunology. This is an open access article under the CC BY license (http://creativecommons.org/licenses/by/4.0/).

https://doi.org/10.1016/j.jaci.2022.08.019

Abbreviations used

AS: Alternative splicing
ASC: Apoptosis-associated speck-like protein containing a caspase recruitment domain
CAPS: Cryopyrin-associated periodic syndromes
CRISPR: Clustered regularly interspaced short palindromic repeat
FL: Full length
GSDMD: Gasdermin D
LPS: Lipopolysaccharide
LRR: Leucine-rich repeats
mRNA: Messenger RNA
NEK7: NIMA-related kinase 7
NLR: Nucleotide-binding and oligomerization domain–like receptor
PBMC: Peripheral blood mononuclear cell
PMA: Phorbol 12-myristate 13-acetate
sg: Single guide
SRA: Sequence read archive
WT: Wild type

introns and exons is rearranged through the differential use of splice sites, providing different mRNA coding sequences from the same gene; therefore, AS is an alternative mechanism of signaling regulation as it increases transcriptome complexity and creates protein diversity. Deregulation of AS is involved in the pathogenesis of cancer, metabolic disorders, and autoimmune diseases such as systemic lupus erythematosus and rheumatoid arthritis.[12] One study suggested that LRR AS may play a regulatory role in NLRP3 activity by interfering with NIMA-related kinase 7 (NEK7) interaction.[9] NEK7 is a mitotic serine/threonine kinase that was suggested to be required for NLRP3 inflammasome activation through direct NLRP3-NEK7 interaction.[13-17]

The LRR of NLRP3 has additional functions that could be affected by AS. SGT1 and HSP90 are chaperones that were found to interact with the LRR region of NLRP3; knockdown of SGT1 or chemical inhibition of HSP90 decreased inflammasome activity, and inhibition of HSP90 reduced NLRP3-mediated gout-like inflammation in mice,[18] suggesting that the LRR sequence may be essential for binding regulatory molecules and control of NLRP3 activation.

The NLRP3 inflammasome plays an important role in autoinflammatory diseases, a group of inflammatory conditions usually present in childhood with recurrent or continuous attacks of fever and systemic inflammation. These pathologies are characterized by exaggerated activation of innate immunity at basal or in response to exogenous or endogenous stimuli. Constitutive inflammasome activation through gain-of-function mutations in the NLRP3-NACHT region promotes excessive IL-1β release and causes autoinflammatory diseases in cryopyrin-associated periodic syndromes (CAPS or cryopyrinopathies).[19,20] CAPS comprise a group of rare autoinflammatory diseases, which has recently served as a model of IL-1β–driven diseases. In addition to inherited autoinflammatory conditions, NLRP3 is involved in various diseases, such as autoimmune disorders, neurodegenerative diseases, gout, diabetes, atherosclerosis, and cancer.[21]

The contribution of AS in NLRP3-LRR to human diseases remains unknown. This study describes the presence of NLRP3-LRR splice variants in steady-state and activated human monocytes. In addition, we investigate the functional role of each LRR-coding exon in natural versus CAPS-induced inflammatory conditions *in vitro*. We identify exon specificity essential for inflammasome assembly and function, demonstrating that the LRR of NLRP3 is required for inflammasome activation in CAPS and suggesting that LRR AS may determine the pathogenic properties of NLRP3 in autoinflammatory diseases.

METHODS

Cloning and plasmids, generation of stable cell lines, immunoblot analysis, cell culture, protein immunoprecipitation, transient transfection in HEK293T cells, ASC oligomerization assay, and RNA isolation and reverse transcription are described in this article's Methods section in the Online Repository available at www.jacionline.org.

Chemicals and antibodies

Ultrapure lipopolysaccharide (LPS) from *Escherichia coli* was purchased from InvivoGen (San Diego, Calif). Nigericin, phorbol 12-myristate 13-acetate (PMA), and MG132 were purchased from Sigma-Aldrich (St Louis, Mo). Monosodium urate crystals were prepared as previously described.[22] Z-Vad-FMK was purchased from Bachem (Bubendorf, Switzerland). 1,4-Dithiothreitol and doxycycline hyclate were from AppliChem (Darmstadt, Germany).

Monoclonal anti-human NLRP3 (dilution 1/1000, AG-20B-0014), caspase-1 (dilution 1/1000, AG-20B-0048), and α-tubulin (dilution 1/1000, AG-27B-0005-C100) antibodies were purchased from AdipoGen (San Diego, Calif). Monoclonal anti-human IL-1β (dilution 1/1000, 12242s), cleaved IL-1β (dilution 1/1000, 83186S) antibodies were purchased from Cell Signaling Technology (Danvers, Mass). Polyclonal anti-human ASC antibodies were purchased from AdipoGen (AL177, dilution 1:1000, AG-25B-0006) and Santa Cruz Biotechnology (Santa Cruz, Calif; dilution 1/200, sc-22514). Monoclonal anti-human GSDMD antibody (dilution 1/1000, EPR19829) was from Abcam (Cambridge, United Kingdom). Monoclonal anti-human SGT1 (dilution 1/2000, 612104) and HSP90 (dilution 1/1000, 610418) antibodies were purchased from BD Bioscience (Franklin Lakes, NJ). Monoclonal anti-FLAG (DYKDDDDK Tag) antibody (dilution 1/2000, A00187) was from GenScript (Nanjing, China). Polyclonal anti-rabbit cross-absorbed secondary IgG Alexa Fluor 647 conjugate antibody was from Thermo Fisher Scientific (Waltham, Mass; dilution 1/1000).

Inflammasome assay

For the priming step, THP1 cells were primed for 3 hours in the presence of 0.5 μmol PMA. U937 cells were primed for 3 hours in the presence of 0.2 μmol PMA or overnight in the presence of 0.1 μmol PMA. Peripheral blood mononuclear cells (PBMCs) were primed with LPS 200 ng/mL for 1 hour, for 4 hours, or overnight. Cells were plated in 12-well plates at a density of 2 × 106 cells per well or in 24-well plates at a density of 1 × 106 cells per well, and incubated at 37°C with 5% CO2.

For the inflammasome activation step, cells were stimulated with 5 μg/mL of nigericin for 30 minutes to 2 hours. U937 cells containing a doxycycline-inducible lentiviral vector plasmid were pretreated with doxycycline 0.3-3 μg/mL for 4 to 24 hours.

Quantitative real-time PCR

Previously synthetized complementary DNA was diluted in diethylpyrocarbonate-treated water. A homemade PCR mix was used containing 50 mmol KCl, 20 mmol Tris-HCl, 2.5 mmol $MgCl_2$, 0.1 mg/mL bovine serum albumin, 0.125 μmol forward primer, 0.125 μmol reverse primer, 250 μmol deoxyribonucleotide triphosphate, 1× SYBR, 25 U/mL Taq polymerase, and each complementary DNA sample in a total volume of 10 μL. PCR was performed in triplicate in 384-well plates using a LightCycler480 Real Time PCR system (Roche, Basel, Switzerland). Samples were normalized using a housekeeping gene (actin). All oligonucleotides were

synthetized by Microsynth AG (Balgach, Switzerland). Primer sequences are listed in Table E1in the Online Repository at www.jacionline.org.

Bioinformatic analysis

Bioinformatic analysis was performed by 'psichomics,' an R package (R Project; www.r-project.org) with a graphical application for AS quantification and analysis. AS quantification in 'psichomics' is based on exon–exon junction read counts. Therefore, 'psichomics' quantifies by default all skipped exon events. For each AS event in a given sample, its percentage spliced in, or PSI, value is estimated by the proportion of exon–exon junction read counts supporting the inclusion isoform.[23]

Statistical analysis

All data are representative of at least 3 different experiments. Statistical significance was ascertained by performing appropriate tests in GraphPad Prism software version 9.1.2 (GraphPad Software, La Jolla, Calif). Significant differences are indicated as $*P \leq .05$, $**P \leq .01$, or $***P \leq .001$.

RESULTS

Pattern of NLRP3 splicing in human monocytes

To investigate the pattern of NLRP3 splice variants in human cells, we analyzed sequence read archive (SRA) data from experiments using human primary monocytes (SRP116937). We identified 14 different variants of NLRP3 within the LRR (Fig 1, *A*). By analyzing the exon–exon junctions, we identify 2 previously unknown splice variants linked to a splicing acceptor site within exon 5. This splicing site creates a cryptic intron (called an exitron) within exon 5 and, upon exitron splicing, generates a new in frame sequence linked to either exon 3 or exon 4. The new sequences are in frame with NLRP3 and generated a truncated protein-coding for exactly one entire LRR in exon 5 (see Fig E1, *A,* in the Online Repository at www.jacionline.org). While many variants were represented at very low frequency in these data sets, the variants skipping exons 4, 5, and 6 were abundantly present and occasionally represented the majority of NLRP3 within the sample, indicating that AS can constitute a significant source of NLRP3 variation. The splicing-induced variability in NLRP3 isoform expression measured in human primary monocytes is shown in Fig 1, *A*. The schematic representation of the most common splice variants is provided as Fig E1, *B*.

To experimentally confirm these observations, we developed a PCR-based technique that detects the most frequent NLRP3 LRR splice variants (Fig 1, *B*). The specificity of PCR primers was validated by DNA sequencing of amplified sequences. Furthermore, the application of this method by real-time PCR confirmed the presence of those variants in PBMCs from healthy donors and CAPS patients, and in monocytic cell lines THP1 and U937 (Fig 1, *C,* and see Fig E2 in the Online Repository at www.jacionline.org).

Exons 4, 5, 7, and 9 are required for inflammasome function

To assess the potential impact of AS on the overall NLRP3 LRR protein conformation, we compared structural models of several NLRP3 LRR splice variants. The models were generated with SWISS-MODEL[24] and visualized with PyMOL software. To model NLRP3-LRR, we used the solved structure of the Ribonuclease Inhibitor (RI: 2bnh.1.A), whose sequence and genomic organization are similar and evolutionarily related to NLRs.[25] The LRR models show an intact overall domain structure in all variants, except for the variant with deletion of the exitron in exon 5, in which the last alpha helix seems to be out of axis, indicating that all NLRP3 variants with one complete exon deletion in the LRR are potentially structurally functional (see Fig E3 in the Online Repository at www.jacionline.org).

To investigate the functional impact of each LRR coding exon in inflammasome activation, we generated *N*-terminally FLAG-tagged NLRP3 constructs for every possible LRR skipped exon in the TET-ON pINDUCER21 vector (+P21),[26] allowing the control of the expression of each NLRP3 variant by doxycycline exposure (Fig 2, *A*). U937, a monocytic cell line competent for inflammasome activation, was edited for endogenous NLRP3 deletion using clustered regularly interspaced short palindromic repeat (CRISPR)/Cas9 targeting the genome with a NLRP3 single guide RNA (sg-NLRP3). NLRP3-deficient cells were reconstituted with +P21 NLRP3 splice variants or a +P21 empty vector control (Fig 2, *A* and *B*). The NLRP3 constructs were engineered with a silent mutation conferring resistance to the sg-NLRP3 CRISPR/Cas9 deletion. Then, for each generated population, we assessed NLRP3 expression and the ability of inflammasome activation. Cells were primed with PMA (signal 1), and expression of the NLRP3 variants was induced using doxycycline. Treatment with nigericin was used to activate inflammasome assembly (signal 2). As expected, NLRP3 deficiency abolished inflammasome activity compared to control cells expressing sg-Luci, an irrelevant sg-RNA (Fig 2, *B*). However, reconstitution of these cells with NLRP3 fully restored inflammasome activation as measured by the release of mature IL-1β, cleaved caspase-1, and cleaved GSDMD (Fig 2, *B*).

To account for the slight difference in expression of the splice variants, we used increasing doses of doxycycline to modulate the expression of all NLRP3 splice variants. Full-length (FL) NLRP3 restored inflammasome function in the presence of nigericin at every dox concentration used in this system (Fig 2, *C*); however, the maximum dose used was sufficient to promote spontaneous inflammasome activation of FL-NLRP3 even in the absence of nigericin. Using this assay, we confirm the previous finding indicating that the Δ4 variant is nonfunctional.[9] In addition, we found that the variants Δ5, Δ7, and Δ9 lose their competence in inflammasome activation, reflected by the absence of IL-1β cleavage detection in the supernatant of cells after nigericin treatment. In contrast, NLRP3 variants Δ6 and Δ8 were able to reconstitute inflammasome activity in this model (Fig 2, *C*), indicating that specific amino acid sequences within individual LRR rather than the length of the total LRR domain control inflammasome assembly and nigericin sensing.

Deletion of exon 4, 5, 7, or 9 abolishes autoinflammasome activation in CAPS

To assess the impact of NLRP3 AS in spontaneous activation and inflammasome assembly, we subcloned the NLRP3 splice variants constructs in a human CAPS model harboring the R262W mutation (also known as R260W), which represents one of the most common autoinflammation-driving CAPS mutations (Fig 3, *A*). We reconstituted NLRP3-deficient U937 cells with the splice variants carrying the CAPS mutation. In this model, induction of NLRP3 is sufficient to drive inflammasome activation independent of additional activating signals. We found that similar to wild-type (WT) NLRP3, CAPS variants Δ6 and Δ8 showed spontaneous inflammasome activity as

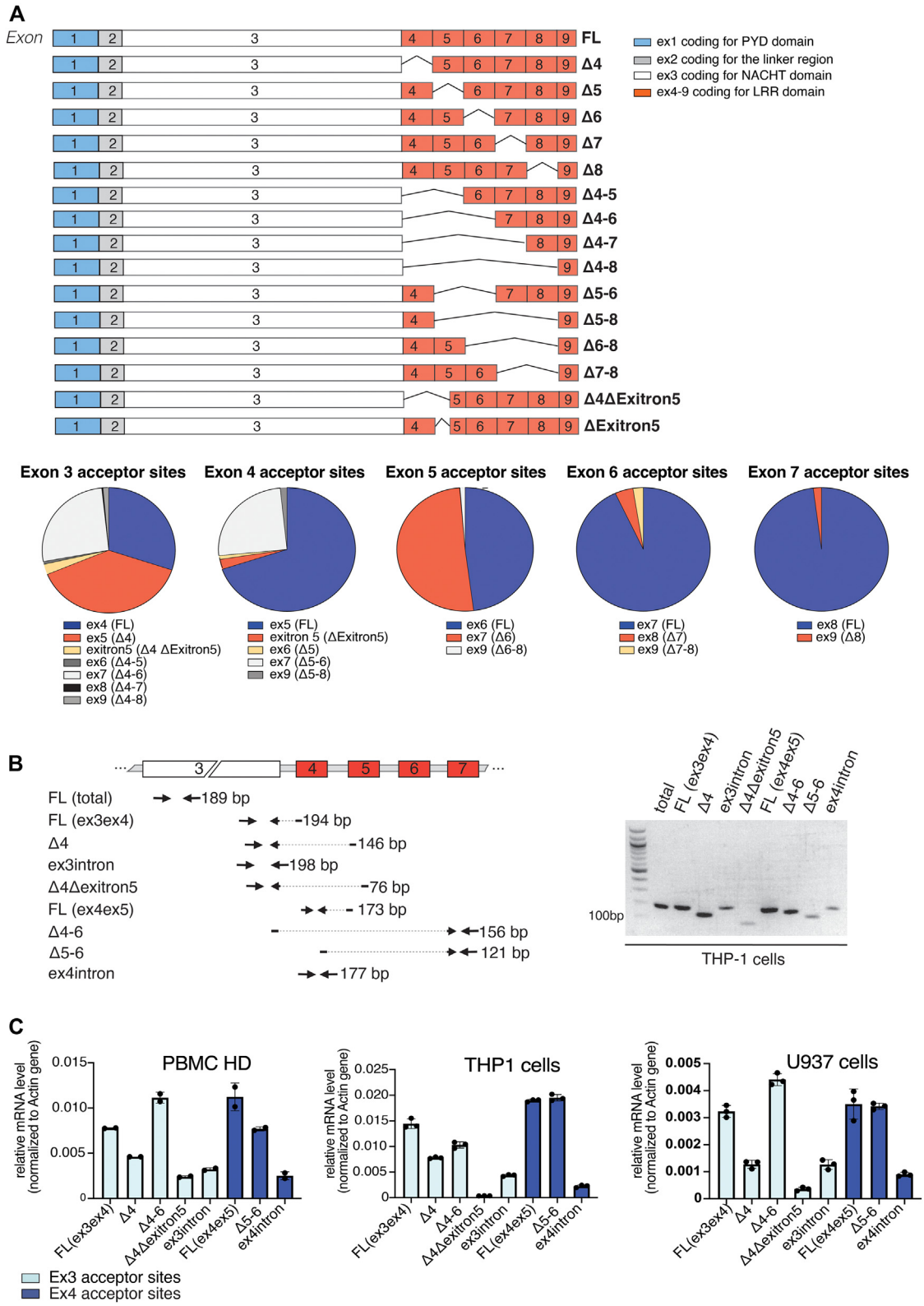

FIG 1. Pattern of NLRP3 splicing in human cells. **(A)** Catalog of NLRP3-LRR splice variants detected in primary human monocytes after bioinformatic analysis of availed SRA data sets (SRP116937). Pie charts show the diversity of NLRP3 alternative exons linked to the donor sites in exons 3, 4, 5, 6, and 7 in untreated human primary monocytes analyzed ex vivo. **(B)** Development of a strategy to detect splice variants in human cells using PCR. The design of the primers used is illustrated. The mRNA expression of NLRP3 splice variants was assessed by PCR in THP1 cells. DNA was extracted and sequenced by the Sanger method from each gel fragment corresponding to a single form of each NLRP3 splice variant. This method is not quantitative and does not account for differences in amplification efficiency and mRNA stability. **(C)** Detection of NLRP3 splice variants in untreated human PBMCs from 5 healthy donors *(HD)* in THP1 cells and in U937 cells by quantitative real-time PCR.

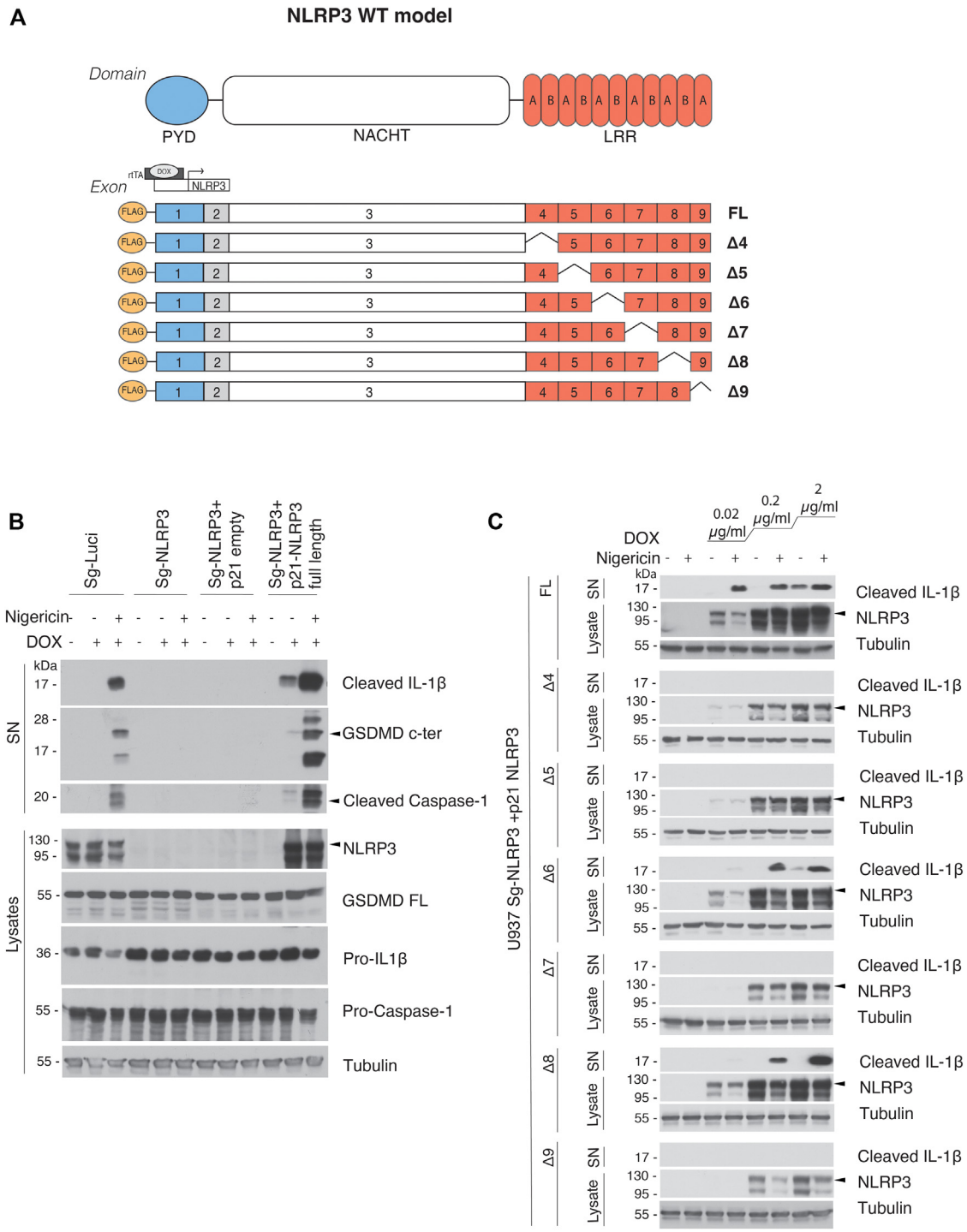

FIG 2. Exons 4, 5, 7, and 9 are required for inflammasome function. **(A)** Schematic representation of *N*-terminally FLAG-tagged NLRP3 constructs for every LRR skipped exon splicing possibility in a human cellular model representing physiologic condition. **(B)** Deletion of NLRP3 in U937 cells using CRISPR/Cas9 and sg-RNA targeting luciferase (sg-Luci) or NLRP3 (sg-NLRP3). Reconstitution of NLRP3-deficient cells with NLRP3-FL in a doxycycline-inducible system (p21) or empty p21 vector. The cells were differentiated with PMA 0.2 μmol for 3 hours, stimulated or not with doxycycline *(DOX)* 0.3 μg/mL for 4 hours, and treated or not with nigericin 5 μg/mL for 2 hours. The expression of NLRP3 and other inflammasome components (pro–caspase-1, GSDMD FL, pro–IL-1β), as well as caspase-1, GSDMD, and IL-1 β cleavage were analyzed by Western blot test in total cell lysates or cell supernatants *(SN)*. Tubulin was used as a loading control. **(C)** NLRP3-deficient U937 cells were reconstituted with NLRP3-WT FL, Δ4, Δ5, Δ6, Δ7, Δ8, and Δ9 splice variants in a doxycycline-inducible p21 vectors. PMA-differentiated cells were stimulated with increasing doses of DOX for 4 hours and treated or not with nigericin 5 μg/mL for 2 hours. NLRP3 expression and IL-1β cleavage were analyzed by Western blot test. Tubulin was used as a loading control.

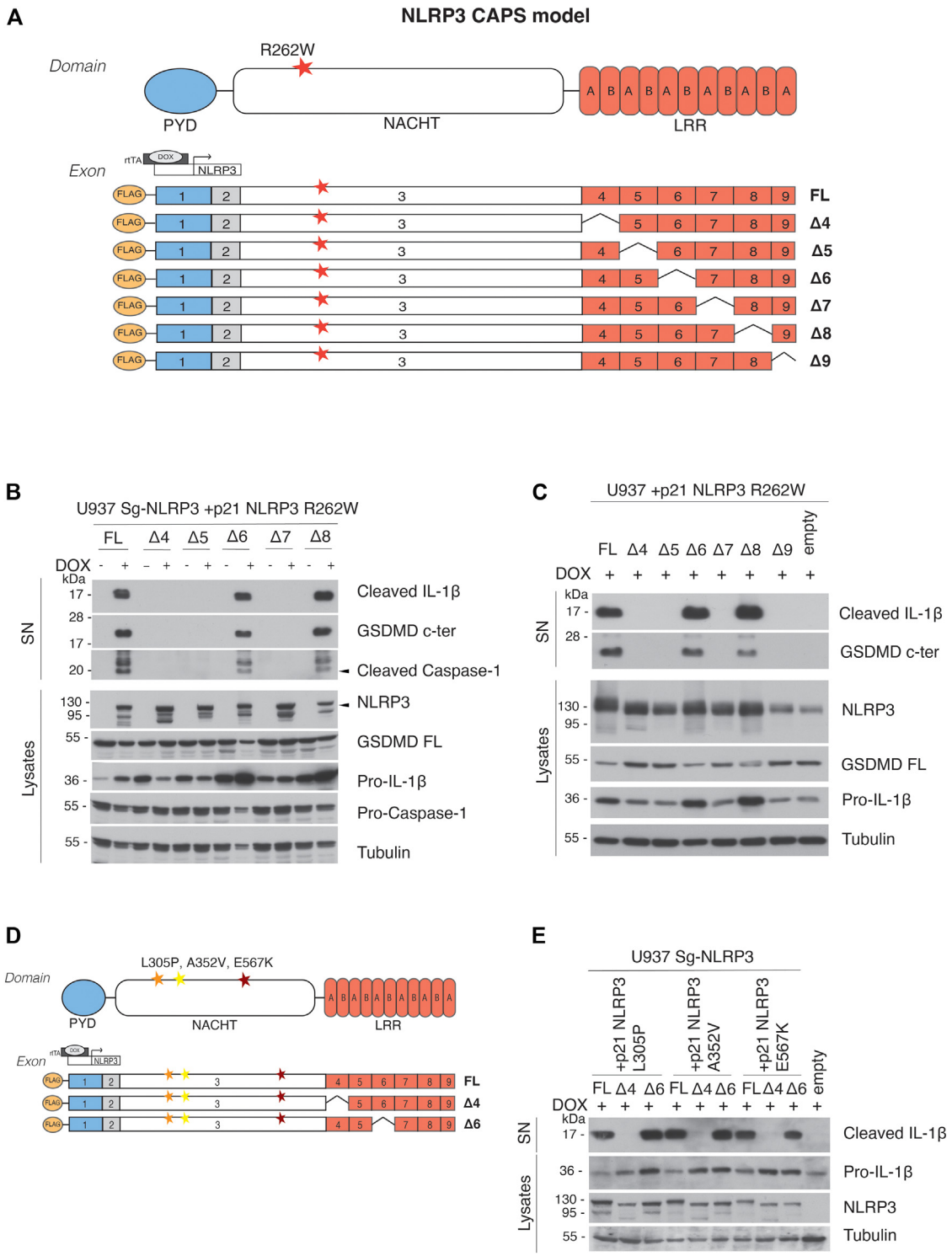

FIG 3. LRR exons 4, 5, 7, and 9 are required for inflammasome activation in CAPS. **(A)** Schematic representation of *N*-terminally FLAG-tagged NLRP3 constructs for every LRR skipped exon splicing possibility in a human cellular model representing CAPS autoinflammatory condition with R262W mutations. **(B)** NLRP3-deficient U937 cells (sg-NLRP3) were reconstituted with NLRP3 R262W FL, Δ4, Δ5, Δ6, Δ7, and Δ8 splice variants in p21 vector. PMA-primed cells were stimulated or not with doxycycline 2 μg/mL for 8 hours. Expression of inflammasome components and cleavage of IL-1β, caspase-1, and GSDMD was assessed by Western blot test. Tubulin was used as a loading control. **(C)** U937 parental cells (expressing endogenous NLRP3) were reconstituted with NLRP3 R262W FL, Δ4, Δ5, Δ6, Δ7, Δ8, and Δ9 splice variants and treated with doxycycline 2 μg/mL for 8 hours and analyzed as in *(B)* (**D** and **E**) Parental U937 cells were reconstituted with NLRP3 FL, Δ4, and Δ6 variants harboring the L305P, A352V, or E567K CAPS mutations. PMA-differentiated cells were stimulated with 2 μg/mL for 8 hours and analyzed as in *(B).*

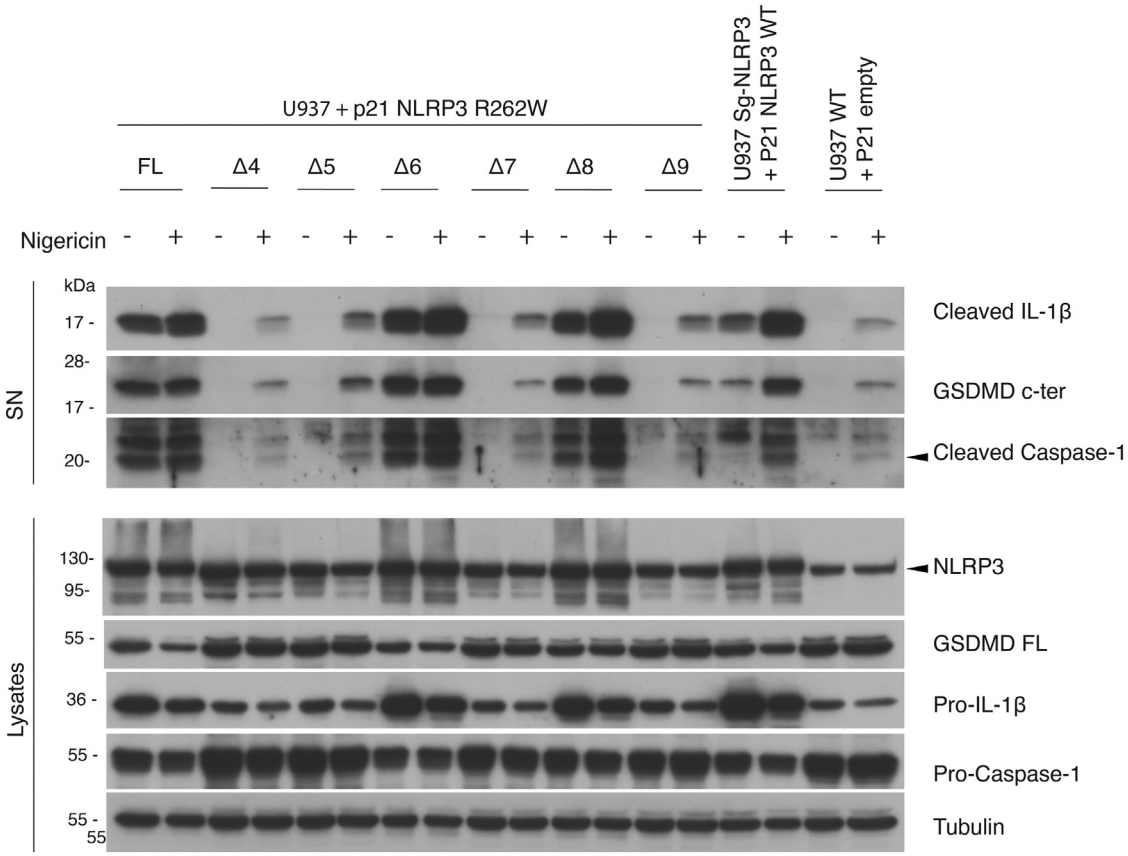

FIG 4. Unfunctional NLRP3 splice variants do not present dominant-negative abilities. U937 parental cells (expressing endogenous NLRP3) reconstituted with NLRP3 R262W FL, Δ4, Δ5, Δ6, Δ7, Δ8, and Δ9 splice variants were differentiated with PMA and stimulated with doxycycline 2 μg/mL for 8 hours and treated or not with nigericin 5 μg/mL for 2 hours. Expression of inflammasome components (NLRP3, pro–caspase-1, GSDMD FL, pro–IL-1β) and cleavage of IL-1β, caspase-1, and GSDMD were assessed by Western blot test. Tubulin was used as a loading control.

measured by the release of its substrates (Fig 3, *B*). Furthermore, the presence of an endogenous WT-NLRP3 allele, as is the case in CAPS patients, did not affect inflammasome functionality of the different CAPS splice variants (Fig 3, *C*). Again, FL, Δ6, and Δ8 were forming active complexes, while none of the other variants lacking exon 4, 5, 7, or 9 could (Fig 3, *C*).

Moreover, we compared inflammasome activation in functional variants FL, Δ6, and Δ8 by ELISA. We found similar levels of cleaved IL-1β release in all functional variants in both the NLRP3-WT and CAPS models (see Fig E4 in the Online Repository at www.jacionline.org), suggesting that the exclusion of exons 6 and 8 do not perturb inflammasome potential.

To confirm the functional role of the splice variants in other CAPS mutations, we generated additional human CAPS models expressing NLRP3 carrying the L305P, A352V, or E567K mutation, in which we subcloned the most common nonfunctional and functional splice variants, Δ4 and Δ6, respectively (Fig 3, *D*). We found that Δ4 was inactive while Δ6 remained competent for inflammasome activation, independent of the CAPS-causing mutation (Fig 3, *E*).

Nonfunctional variants do not compete with competent variants

Because CAPS are autosomal-dominant diseases, we reasoned that inactive CAPS splice variants could affect the activity of WT alleles. To address this question, we took advantage of the generated population expressing endogenous WT allele and dox-inducible CAPS variants. We treated these cells with nigericin and analyzed inflammasome activity. In this context, the additional cleavage observed after treatment with nigericin reflects the endogenous NLRP3 cleavage.

We found that endogenous NLRP3-driven cleavage of IL-1β, GSDMD, and caspase-1 was not affected by the expression of nonfunctional CAPS variants (Δ4, Δ5, Δ7, Δ9) compared to the levels of substrate cleavage observed in cells reconstituted with empty vector (Fig 4). These data suggest that nonfunctional LRR variants do not behave as dominant negative and do not impair activation of WT-NLRP3 by natural ligands.

Inactive variants cannot trigger ASC polymerization

To evaluate if the inflammasome defects observed in the nonfunctional NLRP3 variants are upstream or downstream of ASC oligomerization, we quantified the formation of ASC specks in NLRP3-deficient U937 cells reconstituted with the CAPS-NLRP3 variants by imaging flow cytometry (Fig 5, *A*, and see Fig E5 in the Online Repository at www.jacionline.org). We confirmed that the Δ6 and the Δ8 variants could trigger ASC oligomerization. However, we observed the absence of significant ASC speck formation in the nonfunctional variants, suggesting

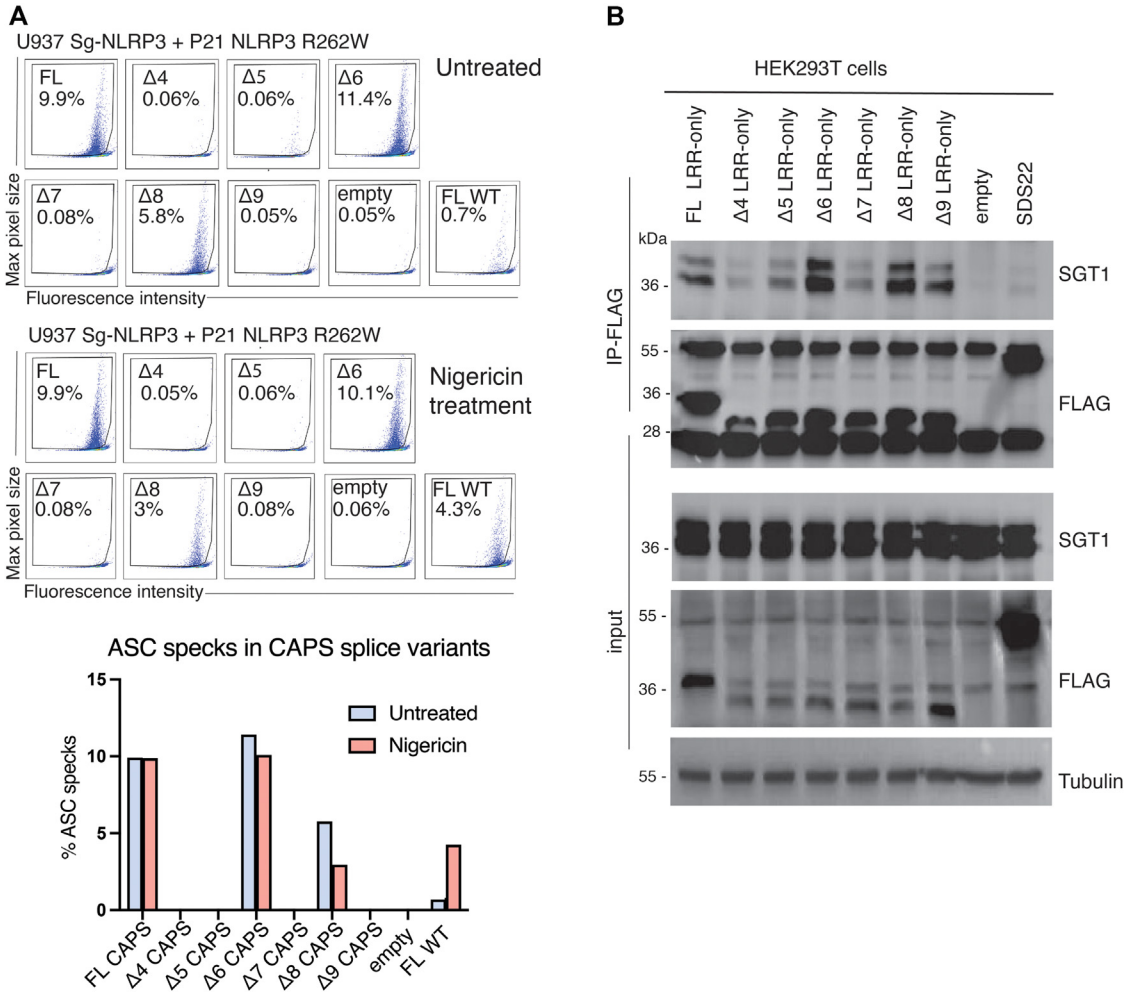

FIG 5. Nonfunctional variants show impaired ASC oligomerization and reduced binding to SGT1. **(A)** Quantification of ASC specks by imaging flow cytometry, in NLRP3-deficient U937 cells (sg-NLRP3) reconstituted with NLRP3 R262W FL, Δ4, Δ5, Δ6, Δ7, Δ8, and Δ9 splice variants, NLRP3-WT-FL or empty vector, in a doxycycline-inducible system. Cells were treated with doxycycline 2 μg/mL for 8 hours and stimulated or not with nigericin 5 μg/mL for 1 hour. Bar chart illustrates the percentage of positive cells for ASC specks in each NLRP3 variant after nigericin treatment or not. **(B)** Transient transfection of HEK293T cells with FLAG-tagged LRR-only constructs (FL, Δ4, Δ5, Δ6, Δ7, Δ8, Δ9), empty vector, and SDS22 (negative control) was performed. Whole lysates were immunoprecipitated with anti-Flag antibodies and analyzed by Western blot test as indicated.

a functional role of the LRR domain upstream of ASC oligomerization (Fig 5, *A*). Furthermore, treatment with nigericin did not affect ASC speck formation in the variants, indicating that the loss of essential exons within the LRR completely blunt spontaneous and stimuli-induced inflammasome formation (Fig 5, *A*).

Functional NLRP3 variants display an increased affinity for SGT1

NLRP3-LRRs were shown to directly bind proteins that regulate NLRP3 activity and inflammasome formation. SGT1 is a molecular chaperone that interacts specifically with the NLRP3-LRR region.[18,27] We therefore investigated whether this interaction was affected among the splice variants. To address this question, we generated *N*-terminally FLAG-tagged LRR-only constructs for NLRP3 coding for the FL-LRR region and the LRR variants (Δ4, Δ5, Δ6, Δ7, Δ8, and Δ9). We transfected these constructs in HEK293T cells and analyzed the interaction between endogenous SGT1 and the LRR splice variants by immunoprecipitation. The LRR-containing protein SDS22 was used as a negative control to exclude the possibility of nonspecific binding of SGT1 to LRR domains. SGT1 interacted preferentially with the LRR domain of functional variants FL, Δ6, and Δ8 (Fig 5, *B*). These data suggest that variation within the LRR directly affects protein–protein interactions upstream of inflammasome assembly.

Selective upregulation of FL-NLRP3 after treatment with inflammasome-modulating molecules

To assess the effect of known inflammatory mediators on NLRP3-AS, we analyzed available SRA data sets. We identified 2 experiments demonstrating treatment-induced variation in NLRP3 splicing. Because we found Δ4 to be the most abundantly present nonfunctional variant, we quantified exon 4 inclusion in RNA sequencing data from PBMCs and monocytes, isolated from

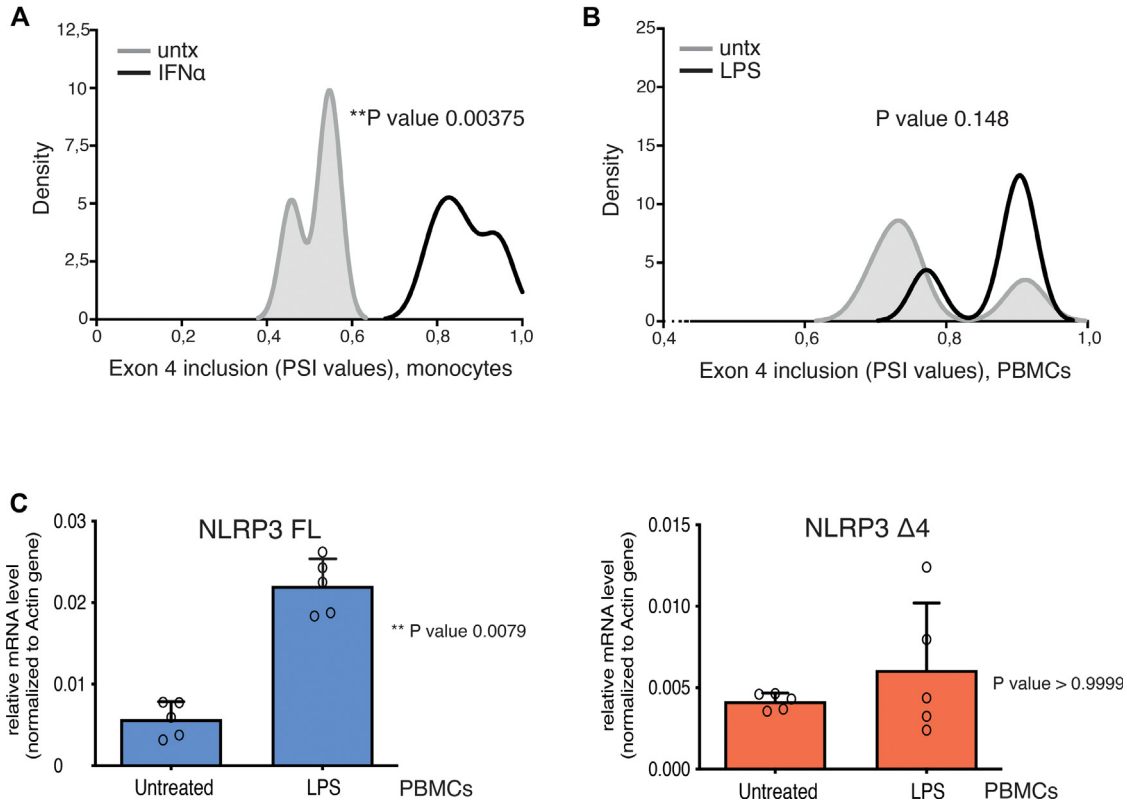

FIG 6. Treatment with LPS selectively upregulates the expression of NLRP3 with exon 4 inclusion. (**A** and **B**) Density plots showing the distribution of the inclusion levels of NLRP3 exon 4 in PBMCs and monocytes, treated or not with LPS for 4 hours and IFN-α for 6 hours, for SRP062958 *(A)* and ERP005301 *(B)*, respectively. Analysis was performed by using the visual interface of the 'psichomics' R package. The percentage spliced in, or PSI, values were estimated by the proportion of exon–exon junction read counts supporting the inclusion of exon 4 in the given samples. Statistical significance was calculated by Welch 2-sample *t* test. **(C)** Human PBMCs isolated from 5 healthy adult donors were treated with LPS 200 ng/mL for 1 hour. The expression of NLRP3 with exon 4 inclusion (FL) or Δ4 was investigated by real-time PCR. Statistical significance was calculated by Mann-Whitney test.

healthy donors, treated or not with IFN-α for 6 hours (ERP005301), or with LPS for 4 hours (SRP062958), respectively. Our analysis demonstrates a decrease in exon 4 exclusion in PBMCs treated with IFN-α (Fig 6, *A*). A similar trend was observed in monocytes treated with LPS compared to those not treated (Fig 6, *B*). To test this possibility, we analyzed exon 4 inclusion in PBMCs from healthy donors treated with LPS. We found that LPS significantly increased the expression of NLRP3 with exon 4 inclusion (FL variant). However, LPS promoted no increase in the Δ4 variant (Fig 6, *C*). These findings indicate that the inflammatory context can modulate the repertoire of NLRP3 toward increased functionality and responsiveness.

DISCUSSION

How the NLRP3-LRR region contributes to inflammasome activation is not fully understood. One study showed that the LRR of human NLRP3 undergoes AS and that the Δ4 variant is inactive.[9] However, the specific role of each LRR coding exon and their implication in the regulation of NLRP3-mediated autoinflammation, such as in the context of CAPS, were not investigated.

In this study, we first confirmed that the LRR domain of NLRP3 is extensively spliced in human monocytes, as expected by its highly conserved, modular, exon–exon organization. We illustrated the pattern of human NLRP3-AS in primary human monocytes and THP1 cells, identifying 2 previously unknown splice variants caused by the presence of an exitron within exon 5. These variants were rare, consistent with the observation that exitrons generally have weak splice sites that can be activated in different tissues or under particular stress conditions.[28] The functionality of the NLRP3 exitron variants is supported by the fact that the junction within exon 5 occurs precisely at the limit between 2 repeats just at the beginning of the LRR type B. Their functionality and possible relevance await further characterization.

Here, we focused on the role of each LRR-coding exon in regulating inflammasome function. Our data indicate that exons 4, 5, 7, and 9 are essential for inflammasome activation, both in the context of NLRP3 sensing of nigericin and in the ligand-independent spontaneous CAPS models. Importantly, we show that excluding exon 6 and exon 8 does not impairs inflammasome activity in any tested models, indicating that the nature of the LRR rather than its length is key for both spontaneous inflammasome activation and responsiveness to NLRP3 agonists. These findings also suggest that NLRP3-AS may regulate conserved activating mechanisms involving the LRR rather than specific ligand-LRR interactions, as CAPS-

mediated autoinflammation is independent of NLRP3 responsiveness to agonists.

Because CAPS is an autosomal-dominant condition, we examined the potential impact of the mutated variants on the WT protein. The absence of any functional repercussion on endogenous NLRP3 demonstrated the absence of dominant-negative properties of the splice variants. This indicates that AS may affect the pool of competent NLRP3 molecules both in CAPS and in physiologic situations without affecting the functionality of FL-NLRP3. Therefore, AS could present a regulatory mechanism of fine-tuning the inflammatory response. In CAPS, NLRP3-AS may explain why, despite the inherited constitutively active NLRP3, patients present variations in the intensity and duration of inflammatory episodes.

SGT1 function in regulating NLRP3 inflammasome activation remains unclear. However, SGT1 is known to bind LRRs in plant NLRs, as well as several human NLRs including NLRP3.[14,18,29] The observation that SGT1 binding to LRR correlates with variant functionality indicates that SGT1 could play a role in inflammasome assembly before oligomerization. NEK7 is another regulator of NLRP3 possibly affected by the variants.[9] NEK7 was shown to be required for NLRP3 inflammasome activation.[13,16,17,30] Here we could not find a direct interaction between NEK7 and LRR. NLRP3 residue Y859, which is located in exon 6 of NLRP3, was experimentally found to be required for NEK7-binding.[13] While we cannot exclude the notion that NEK7 interaction could be affected in the variants, the variant with exon 6 deletion was fully functional in all models tested, suggesting that disrupting NEK7 interaction is not a limiting factor for activation in these settings.

Limitations

The regulation of NLRP3-AS remains a critical question with potential therapeutic implications in autoinflammatory conditions. Our analysis indicated a selective upregulation of the functional FL-NLRP3, while the nonfunctional Δ4 variant remained unchanged, after treatment with inflammatory molecules such as LPS. However, the physiologic relevance of NLRP3 splicing and the protein expression levels for each variant in the patient's tissues remain to be investigated. Our observations suggest that an inflammatory environment could modulate and augment the pool of functional NLRP3 by directing the synthesis of FL-NLRP3. Whether this mechanism could maximize inflammation in the context of infections needs to be investigated. Similarly, we can speculate that splicing regulation of NLRP3 could contribute to initiating or regulating flare duration and intensity in CAPS patients.

The mechanisms by which SGT1 regulates the various NLRP3 variants is also still unclear. In this study, we correlate LRR binding to NLRP3 activity. However, how SGT1 modulates inflammasome assembly is unknown. Future studies aimed at defining SGT1 function may identify new steps involved in NLRP3 regulation.

Conclusion

This study provides insight into NLRP3 inflammasome activation as it defines regions within the LRR domain required for inflammasome function, in both spontaneous, disease-associated inflammasome activation and in NLRP3 responsiveness to agonists.

We thank the staff members of the flow cytometry facility at the University of Lausannefor their help and support with speck experiments.

Key message

NLRP3-AS affects inflammasome assembly, thereby modulating autoinflammation in CAPS models.

REFERENCES

1. Martinon F, Mayor A, Tschopp J. The inflammasomes: guardians of the body. Annu Rev Immunol 2009;27:229-65.
2. Broz P, Dixit VM. Inflammasomes: mechanism of assembly, regulation and signalling. Nat Rev Immunol 2016;16:407-20.
3. Guo H, Callaway JB, Ting JP. Inflammasomes: mechanism of action, role in disease, and therapeutics. Nat Med 2015;21:677-87.
4. Martinon F, Burns K, Tschopp J. The inflammasome: a molecular platform triggering activation of inflammatory caspases and processing of proIL-beta. Mol Cell 2002;10:417-26.
5. Liu X, Zhang Z, Ruan J, Pan Y, Magupalli VG, Wu H, et al. Inflammasome-activated gasdermin D causes pyroptosis by forming membrane pores. Nature 2016;535(7610):153-8.
6. Spel L, Martinon F. Inflammasomes contributing to inflammation in arthritis. Immunol Rev 2020;294:48-62.
7. Swanson KV, Deng M, Ting JP. The NLRP3 inflammasome: molecular activation and regulation to therapeutics. Nat Rev Immunol 2019;19:477-89.
8. Kobe B, Deisenhofer J. Crystal structure of porcine ribonuclease inhibitor, a protein with leucine-rich repeats. Nature 1993;366(6457):751-6.
9. Hoss F, Mueller JL, Rojas Ringeling F, Rodriguez-Alcazar JF, Brinkschulte R, Seifert G, et al. Alternative splicing regulates stochastic NLRP3 activity. Nat Commun 2019;10:3238.
10. Martinon F, Tschopp J. Inflammatory caspases and inflammasomes: master switches of inflammation. Cell Death Differ 2007;14:10-22.
11. Alt FW, Bothwell AL, Knapp M, Siden E, Mather E, Koshland M, et al. Synthesis of secreted and membrane-bound immunoglobulin mu heavy chains is directed by mRNAs that differ at their 3′ ends. Cell 1980;20:293-301.
12. Ren P, Lu L, Cai S, Chen J, Lin W, Han F. Alternative splicing: a new cause and potential therapeutic target in autoimmune disease. Front Immunol 2021;12:713540.
13. Sharif H, Wang L, Wang WL, Magupalli VG, Andreeva L, Qiao Q, et al. Structural mechanism for NEK7-licensed activation of NLRP3 inflammasome. Nature 2019;570(7761):338-43.
14. Shirasu K. The HSP90-SGT1 chaperone complex for NLR immune sensors. Annu Rev Plant Biol 2009;60:139-64.
15. Gaidt MM, Ebert TS, Chauhan D, Schmidt T, Schmid-Burgk JL, Rapino F, et al. Human monocytes engage an alternative inflammasome pathway. Immunity 2016;44:833-46.
16. He Y, Zeng MY, Yang D, Motro B, Nunez G. NEK7 is an essential mediator of NLRP3 activation downstream of potassium efflux. Nature 2016;530(7590):354-7.
17. Shi H, Wang Y, Li X, Zhan X, Tang M, Fina M, et al. NLRP3 activation and mitosis are mutually exclusive events coordinated by NEK7, a new inflammasome component. Nat Immunol 2016;17:250-8.
18. Mayor A, Martinon F, De Smedt T, Petrilli V, Tschopp J. A crucial function of SGT1 and HSP90 in inflammasome activity links mammalian and plant innate immune responses. Nat Immunol 2007;8:497-503.
19. Church LD, Cook GP, McDermott MF. Primer: inflammasomes and interleukin 1beta in inflammatory disorders. Nat Clin Pract Rheumatol 2008;4:34-42.
20. Booshehri LM, Hoffman HM. CAPS and NLRP3. J Clin Immunol 2019;39:277-86.
21. Mangan MSJ, Olhava EJ, Roush WR, Seidel HM, Glick GD, Latz E. Targeting the NLRP3 inflammasome in inflammatory diseases. Nat Rev Drug Discov 2018;17:588-606.
22. Martinon F, Petrilli V, Mayor A, Tardivel A, Tschopp J. Gout-associated uric acid crystals activate the NALP3 inflammasome. Nature 2006;440(7081):237-41.
23. Saraiva-Agostinho N, Barbosa-Morais NL. Psichomics: graphical application for alternative splicing quantification and analysis. Nucleic Acids Res 2019;47:e7.
24. Waterhouse A, Bertoni M, Bienert S, Studer G, Tauriello G, Gumienny R, et al. SWISS-MODEL: homology modelling of protein structures and complexes. Nucleic Acids Res 2018;46(W1):W296-303.

25. Hofsteenge J, Kieffer B, Matthies R, Hemmings BA, Stone SR. Amino acid sequence of the ribonuclease inhibitor from porcine liver reveals the presence of leucine-rich repeats. Biochemistry 1988;27:8537-44.
26. Meerbrey KL, Hu G, Kessler JD, Roarty K, Li MZ, Fang JE, et al. The pINDUCER lentiviral toolkit for inducible RNA interference *in vitro* and *in vivo*. Proc Natl Acad Sci U S A 2011;108:3665-70.
27. Xu G, Fu S, Zhan X, Wang Z, Zhang P, Shi W, et al. Echinatin effectively protects against NLRP3 inflammasome-driven diseases by targeting HSP90. JCI Insight 2021;6:e134601.
28. Marquez Y, Hopfler M, Ayatollahi Z, Barta A, Kalyna M. Unmasking alternative splicing inside protein-coding exons defines exitrons and their role in proteome plasticity. Genome Res 2015;25:995-1007.
29. da Silva Correia J, Miranda Y, Leonard N, Ulevitch R. SGT1 is essential for Nod1 activation. Proc Natl Acad Sci U S A 2007;104:6764-9.
30. Schmid-Burgk JL, Chauhan D, Schmidt T, Ebert TS, Reinhardt J, Endl E, et al. A genome-wide CRISPR (clustered regularly interspaced short palindromic repeats) screen identifies NEK7 as an essential component of NLRP3 inflammasome activation. J Biol Chem 2016;291:103-9.

METHODS

Cloning and plasmids

Generation of pENTR1A-NLRP3 splice variants. FLAG-tagged NLRP3-FL and Δ4 plasmids in PCR-3 vector, generated in our laboratory, were subcloned in the *Bam*H1 and *Xba*I sites of pENTR1A (Invitrogen; Thermo Fisher Scientific) vector.

The point mutation C213A was performed in exon 1 of NLRP3 using PFU DNA polymerase (Agilent Technologies, Santa Clara, Calif) according to the QuikChange site-directed mutagenesis kit, in order to obtain resistance in Cr NLRP3 (oligonucleotide 1; Table E2).

The LRR region was isolated after digestion in *Bgl*II and *Xba*I sites, and a double PCR technique was used for the depletion of each LRR-coding exon. Oligonucleotides 2-11 were used for the first PCR series and oligonucleotide 12 for double PCR (Table E2). All constructs were ligated again to the pENTR1A-NLRP3 plasmid through the same sites (*Bgl*II, *Xba*I).

Generation of LRR-only and NACHT-only constructs. LRR-only and NACHT-only constructs were generated after PCR amplification of the LRR and NACHT fragments of each pENTR1A-NLRP3 plasmid. Phusion HF DNA polymerase (BioLabs, Cambridge, Mass) and oligonucleotides 13-16 (Table E2) were used for the amplification. For each reaction, we used 1 μL of each primer (10 μmol), 10 ng of plasmid, 4 μL of 5× Phusion buffer, 0.4 μL deoxyribonucleotide triphosphate (dNTP), 0.2 μL of Phusion HF DNA polymerase, and H_2O in order to obtain a total volume of 20 μL. PCR-amplified fragments were subcloned in *Bam*HI and *Xba*I sites of Flag-containing pENTR1A vector.

Generation of CAPS constructs. Point mutations were performed in pENTR1A-NLRP3 constructs in order to introduce the CAPS mutations R262W, L305P, L353P, and E567K oligonucleotides 17, 18, 19, and 20, respectively (Table E2). PFU DNA polymerase (from Agilent for R260W mutation and from Promega [Madison, Wis] for the other mutations) was used according to the QuikChange site-directed mutagenesis kit (Stratagene, San Diego, Calif). All constructs were sequenced with adequate primers by Microsynth AG.

Generation of stable cell lines

LentiCRISPR-v2 for NLRP3 targeting. Optimized CRISPR target sequences were cloned into the lentiCRISPR-v2 vector (Addgene, Cambridge, Mass; catalog 52961). CRISPR sequences were designed online by 'benchling' (https://www.benchling.com/crispr/). A sequence targeting luciferase was used as control sg-RNA. The sense and antisense oligonucleotides were designed to incorporate into the restriction enzyme site *Bsm*BI of lentiCRISPR-v2 expressing Cas9 and sg-RNA. Oligonucleotides 21 and 22 were used to target NLRP3 and the luciferase gene, respectively, in order to generate CRISPR-knockout genes (Table E2).

To produce the lentivirus, 2×10^6 293T cells were plated in T175 cm^2 culture flasks in 25 mL complete medium (Dulbecco modified Eagle medium [DMEM], 10% fetal bovine serum [FBS], 1% P/S). Three days after, cells were transfected with 40 μg of the plasmid of interest, 30 μg of pSPAX2, 20 μg of pCMV-VSV-G, 90 μL of transfection reagent PEI, and 3 mL of Opti-MEM in 12 mL of DMEM containing 10% FBS for 12 hours. The day after transfection, medium was replaced with 15 mL of Opti-MEM. On the third day, medium was collected and replaced with 15 mL of Opti-MEM. On the fourth day, viral medium was filtrated using a 0.2 μm filter. Volume was adjusted with 7.5 mL of phosphate-buffered saline (PBS), 1.3 mL of NaCl 5 mol, and 8 mL of polyethylene glycol (PEG 8000, AppliChem). Medium was kept overnight at 4°C on a rotating wheel. The day after, medium was centrifuged for 1 hour at 4000 rpm at 4°C. The supernatant was discarded, and the pellet was resuspended in 200 μL of PBS and kept at −80°C until infection. We used 40 μL of virus preparation to infect the cells. Positive populations were selected with 2-3 μg/mL puromycin for 15 days. NLRP3 expression was assessed by immunoblotting. To obtain full knockout cell lines, the population was cloned by limit dilution and tested again by immunoblotting.

Doxycycline-inducible expression system. Human NLRP3 constructs were subcloned into the pENTR-1A dual selection vector (Invitrogen) and then inserted by LR reaction in a pINDUCER21,[E1] a doxycycline-inducible lentiviral vector plasmid. The expression of NLRP3 was induced with a Tet-On system that uses tetracycline-responsive reverse transcriptional activator (rtTA). The rtTA protein binds to the tetracycline-responsive element in the promoter and activates transcription of a transgene in a doxycycline-dependent manner.

Lentiviruses were produced as previously described by transfecting 293T cells with 40 μg of the plasmid of interest and 10 μg of each packaging plasmid (Tat, Rev, gag/pol, Vsvg). A total of 40 μL of virus preparation was used to infect U937 CR-NLRP3 cells. Positive cells were selected by cell sorting using the green fluorescent protein tag present in the pINDUCER21 by cell sorting.

Immunoblot analysis

After stimulation, supernatant was collected and proteins precipitated by the methanol/chloroform method. Cells were directly lysed in sodium dodecyl sulfate loading buffer (10% glycerol, 2% sodium dodecyl sulfate, 50 mmol Tris-HCl pH 6.8, 12.5 mmol EDTA, 0.02% bromophenol blue) containing 100 mmol of dithiothreitol. Samples were centrifuged for 2 to 5 minutes at 13,000 rpm, then sonicated (10 seconds, 10 pulses) and heated for 5 minutes at 95°C. They were loaded on sodium dodecyl sulfate–polyacrylamide gels for electrophoresis (Axon Laboratory, Scottsdale, Ariz) at 80-140 V and blotted on a Hybond ECL nitrocellulose membrane (Amersham Pharmacia Biotech, Piscataway, NJ) for 1 hour and 30 minutes at 100 V. Membranes were stained with Ponceau S red to monitor protein loading and blocked for 30 minutes at room temperature (RT) with 0.5% Tween and 5% nonfat dry milk in PBS. Membranes were incubated overnight at 4°C with primary antibodies diluted in blocking buffer containing 0.02% of sodium azide. Membranes were washed 3 times for 15 minutes in PBS containing 0.5% Tween and incubated with secondary antibody coupled with peroxidase (1/5000 in blocking buffer, 1 hour, RT). After washing, the signal was detected by membrane incubation for 1 minute with enhanced chemiluminescence reagents (Amersham). Membranes were subsequently exposed to X-ray film (Fuji, Tokyo, Japan) and developed in a darkroom.

Cell culture

U937 and THP1 human monocytic cells lines were cultured in RPMI 1640 (Gibco, Thermo Fisher Scientific) supplemented with 10% FBS. Primary human cells were isolated from blood using Ficoll gradient centrifugation to obtain PBMCs, which were cultured in RPMI 1640 supplemented with 10% FBS. HEK293T cells were cultured in DMEM (Gibco) supplemented with 10% FBS. All cells were grown at 37°C with 5% CO_2. Cells were tested regularly for mycoplasma contamination during the study.

Protein immunoprecipitation

Cells were washed with PBS and lysed in 250 μL immunoprecipitation lysis buffer (20 mmol Tris-HCl pH 7.4, 150 mmol NaCl, 0.2% NP-40, complete protease inhibitor [Roche], and phosphatase inhibitors [NaF, $Na_4P_2OP_7$, Na_3VO_4]) for 30 minutes on ice. Nuclei and membranes were removed by centrifugation (5 minutes, 13,000 rpm). Supernatants were recovered and precleared with Sepharose 6B beads (20 μL per sample, Sigma) for 30 minutes at 4°C. FLAG-tagged NLRP3 was immunoprecipitated using anti-Flag M2 agarose beads (15 μL per sample, Sigma). Immunoprecipitation was performed for 4 hours at 4°C.

Quantification of binding bands was performed by ImageJ (version 2.0.0-rc-69/1.52p) software (https://imagej.nih.gov/ij/).

Transient transfection in HEK293T cells

A total of 4×10^6 HEK293T cells was plated in 60.1 cm^2 culture petri dishes in 10 mL complete medium (DMEM, 10% FBS, 1% P/S). The day after, cells were transfected with 5 μg of the plasmid or plasmids of interest, 15 μL of transfection reagent PEI, and 500 μL of Opti-MEM for 12 to 24 hours at 37°C with 5% CO_2.

ASC oligomerization assay

A total of 4×10^6 U937 cells of each genetically modified sg-NLRP3 U937 cell line (+P21 NLRP3 R260W FL, +P21 NLRP3 R260W Δ4, P21 NLRP3 R260W Δ5, +P21 NLRP3 R260W Δ6, +P21 NLRP3 R260W Δ7, +P21 NLRP3 R260W Δ8, +P21 NLRP3 R260W Δ9, +P21 NLRP3 FL, +P21 empty) were plated in 6-well plates in 2 mL of RPMI 1640 with 10% FBS, doxycycline 2 μg/mL, and Z-Vad-FMK 5 μmol. The next day, the cells were treated or not with nigericin 5 μg/mL for 1 hour.

After stimulation, the cells were collected in 2 mL tubes and centrifuged for 5 minutes at 500 relative centrifugal fields (rcf). The supernatants were discarded, and the pellets were resuspended in 200 μL PBS and transferred to a 96-well plate. The samples were centrifuged again for 5 minutes at 500 rcf. The supernatants were discarded and the pellets were resuspended in 100 μL of fixation solution (BD Cytofix/Cytoperm) and left for 30 minutes at RT. All samples were washed 3 times with 100-200 μL of BD Perm/Wash buffer and centrifuged for 2 minutes at 2000 rpm (4°C). Pellets were resuspended in 200 μL of primary antibody for ASC (dilution 1/200) for 30 minutes. The samples were washed again 3 times with 100-200 μL of BD Perm/Wash buffer and centrifuged for 2 minutes at 2000 rpm (4°C). The pellets were resuspended in 200 μL of secondary antibody (anti-rabbit IgG Alexa Fluor 647 conjugate antibody, dilution 1/1000) for 30 minutes. After 3 more washes as in the previous steps, Hoechst stain was added (dilution 1/2000, 200 μL per well) for 5 minutes. The samples were centrifuged for 2 minutes at 2000 rpm (4°C), the supernatants were discarded, and the pellets were resuspended in 100 μL PBS and stored at 4°C until imaging flow cytometry analysis (Amnis ImageStream^x Mark II; Luminex, Austin, Tex).

RNA isolation and reverse transcription

Total RNA from cells was extracted with Trizol (Invitrogen) or peqGold TriFast (Peqlab, Erlangen, Germany) according to the manufacturers' instructions. For reverse transcription (complementary DNA synthesis), 10 μL of RNA (0.5-2 μg of RNA) sample diluted in diethylpyrocarbonate-treated water was mixed with 10 μL of 2× Reverse Transcription Master Mix (Applied Biosystems, Thermo Fisher Scientific). The 2× Reverse Transcription Master Mix contains 2× RT buffer, 2× RT random primers, 8 mmol of dNTP mix, and 5 U/μL multiscribe reverse transcriptase. The reverse transcription PCR program consisted of the following steps: 10 minutes at 25°C, 120 minutes at 37°C, and 5 minutes at 85°C.

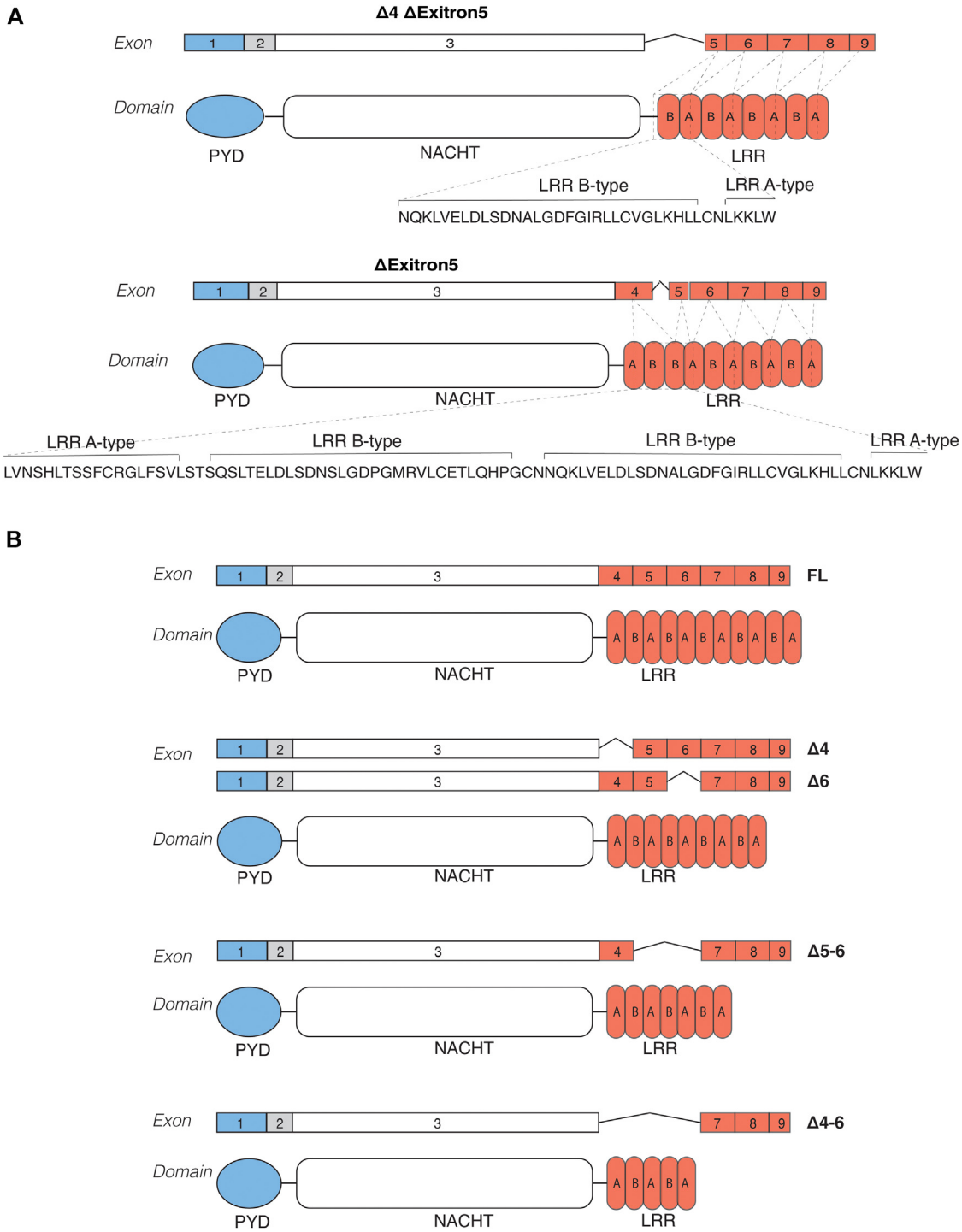

FIG E1. Schematic representation of NLRP3 splice variants. Schematic representation of Δ4 ΔExitron5 and ΔExitron5 variants **(A)** and of the most abundant NLRP3 splice variants identified in human monocytes **(B)**. Both genomic organization in exons and affected translated protein region are represented.

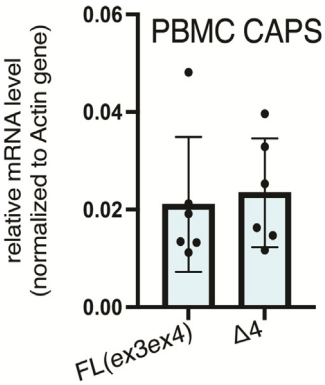

FIG E2. NLRP3-FL and Δ4 are present in PBMCs from CAPS donors. Detection of NLRP3 representative splice variants (FL or missing exon 4, Δ4) in human PBMCs from 5 CAPS donors by quantitative real-time PCR.

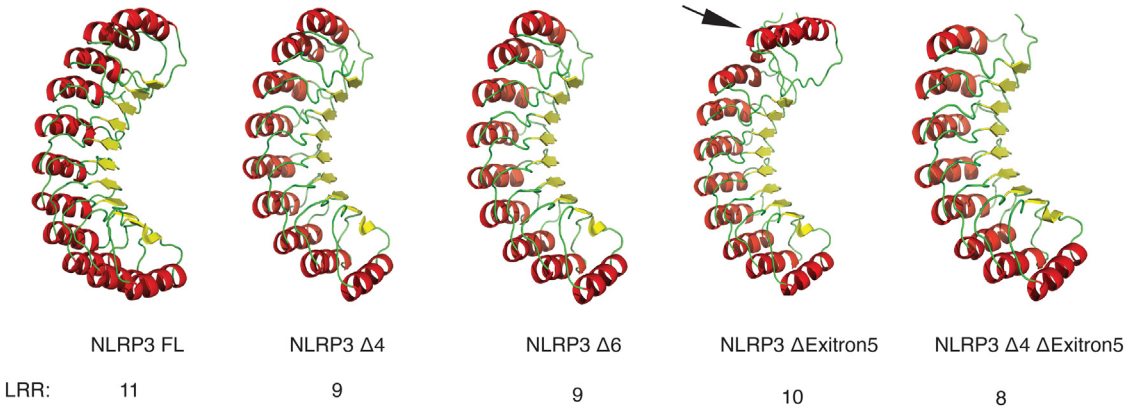

FIG E3. Splicing does not affect the overall domain structure. NLRP3-LRR structural models were generated by SWISS-MODEL using the structure of ribonuclease inhibitor (RI: 2bnh.1.A) and visualized by PyMOL software. Splicing is not predicted to affect the overall structure, except for the NLRP3 ΔExitron5, in which the last alpha axis seems to be out of axis *(arrow).*

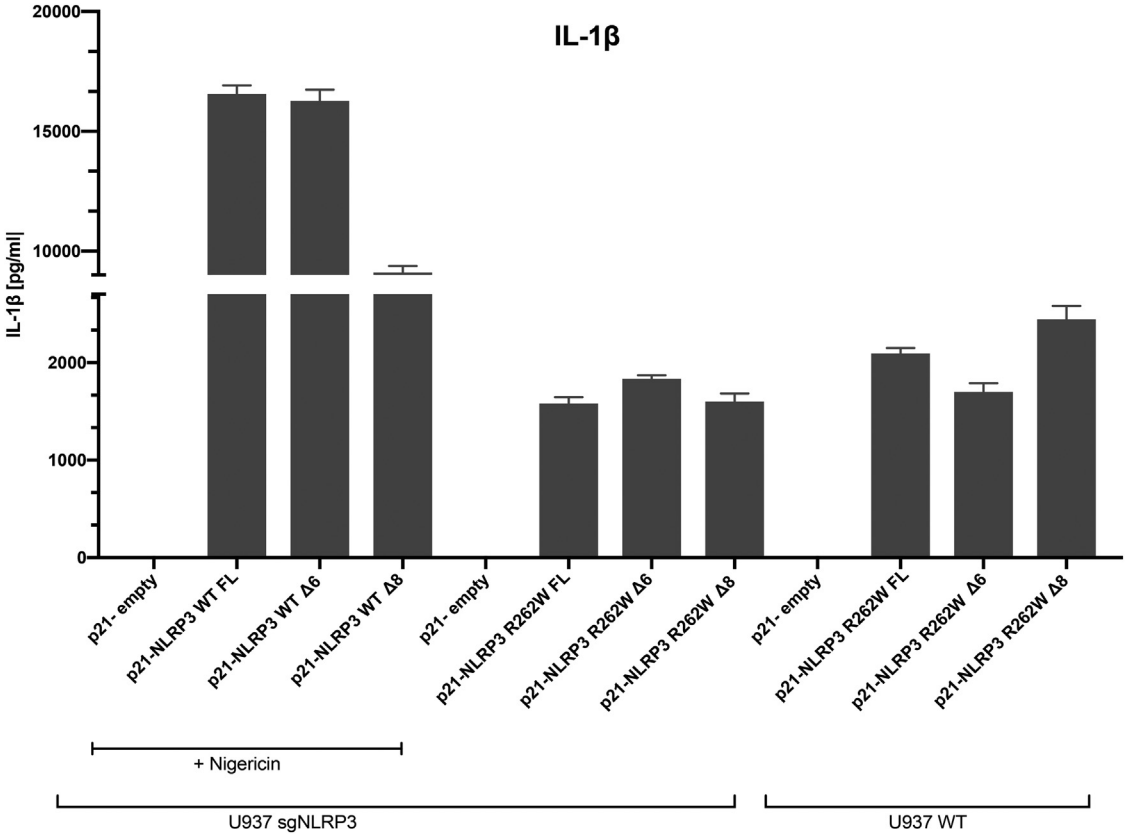

FIG E4. Activation of functional variants Δ6 and Δ8 do not lead to increased inflammasome activation compared to FL. IL-1β release was quantified by ELISA in NLRP3-deficient U937 cells (sg-NLRP3) reconstituted with NLRP3-WT or NLRP3 R262W FL, Δ6, or Δ8 splice variants, and in U937 cells expressing the endogenous NLRP3 (U937-WT) reconstituted with NLRP3 R262W FL, Δ6, or Δ8 splice variants. Cells were treated with doxycycline 2 μg/mL and PMA overnight. U937 sg-NLRP3 cells expressing p21-empty, NLRP3-WT FL, Δ6, and Δ8 constructs were treated with nigericin 5 μg/mL for 1 hour to activate inflammasome.

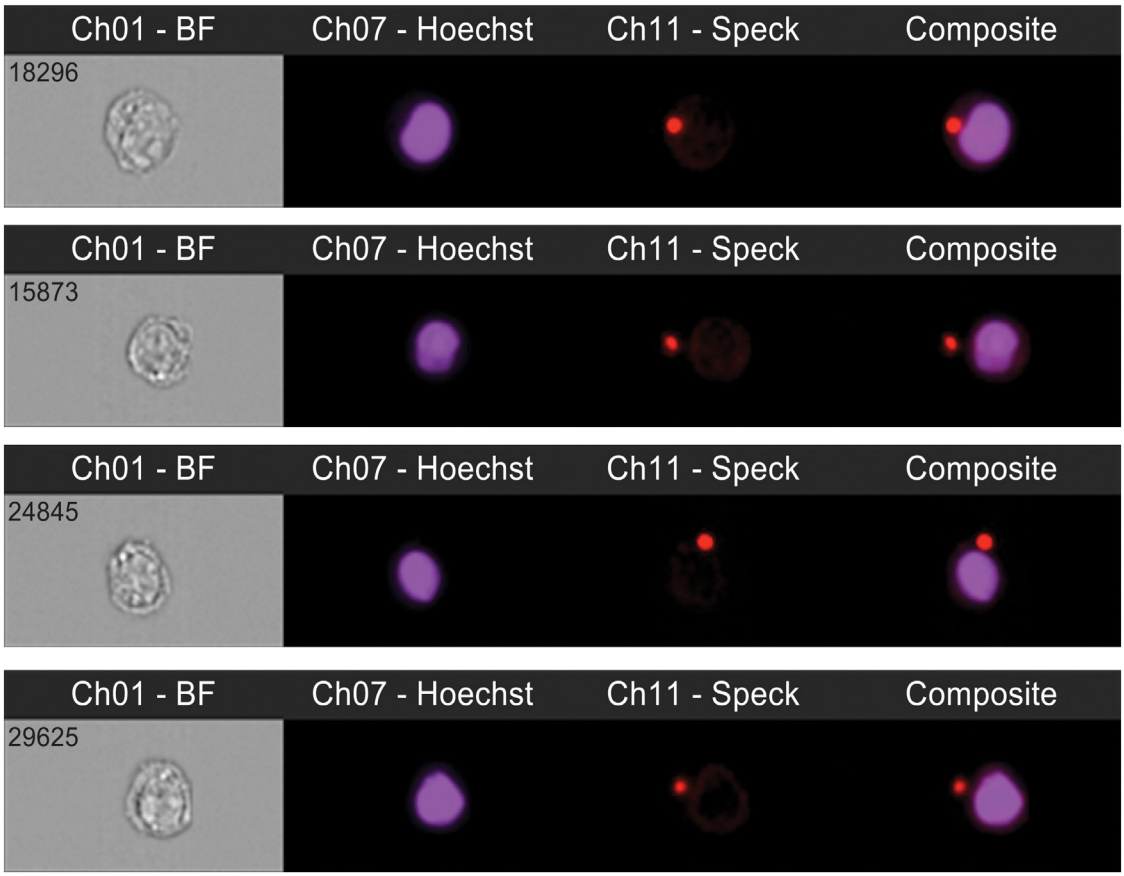

FIG E5. Imaging flow cytometric analysis of ASC specks. Representative images of U937 cells are stained with Hoechst in *purple* (DNA) and ASC in *red.* The *red dot* represent ASC oligomers.

TABLE E1. Primers used for real-time PCR of splice variants

Gene	Forward (5′-3′)	Reverse (5′-3′)
Actin	TACCACCATGTACCCAGGCA	CTCAGGAGGAGCAATGATCTTGAT
NLRP3FL(ex3-ex4)	CCACCAGAATGGACCACAT	GTTCACCAATCCATGAGAAC
NLRP3Δ4	CATCGGGTGGAGTCACTGTC	CGCCCCAACCCATGAGAAC
NLRP3Δ4Δexitron5	AGGCCGACACCTTGATATGG	CTTCTGGTTGCCATGAGAAC
NLRP3ex3intronex4	CTCCACCAGAATGGACCACA	GAGTTTCCTTACCCATGAGAAC
NLRP3Δ4-6	GTTCTCATGGGTTGGTGAATTC	GGTGCAAGAGTCCCTCACAG
NLRP3FL(ex4-ex5)	ACAGCCACCTCACTTCCAGT	GCGCCCCAACCACAATCTCC
NLRP3Δ5-6	GGAGATTGTGGTTGGTGAATTC	TTGTCTCCGAGAGTGTTGCC
NLRP3ex4intronex5	TGGTTTGGAACAGCCACCTC	GGGGACTCACCACAATCTCC
NLRP3total(ex3)	CGTGAGTCCCATTAAGATGGAGT	CCCGACAGTGGATATAGAACAGA

TABLE E2. Oligonucleotides used for cloning

Oligo	Mutation/amplified fragment	Oligo 1 (5′-3′)	Oligo 2 (5′-3′)
1	NLRP3 C213A	CGT GGG CCA TGG CAG TGT GGA TCT TCG	CGA AGA TCC ACA CTG CCA TGG CCC ACG
2	NLRP3 Δ5 product A	AAA AGA TCT CTC AGC AAA TCA GGC TGG AG	AAA TGA CCA ACC ACA ATC TCC GAA TGT
3	NLRP3 Δ5 product B	AAA TCT AGA CTA GTC ATC TAC TCG AG	AAA AGA TTG TGG TTG GTC AGC TGC TGC
4	NLRP3 Δ6 product A	AAA AGA TCT CTC AGC AAA TCA GGC TGG AG	AAA TCA CCA ACC AGA GCT TCT TCA GAT
5	NLRP3 Δ6 product B	AAA TCT AGA CTA GTC ATC TAC TCG AG	AAA AAG CTC TGG TTG GTG AAT TCT GGC
6	NLRP3 Δ7 product A	AAA AGA TCT CTC AGC AAA TCA GGC TGG AG	AAA TGT CTA ATC CCA GTT TCT GCA GGT
7	NLRP3 Δ7 product B	AAA TCT AGA CTA GTC ATC TAC TCG AG	AAA AAA CTG GGA TTA GAC AAC TGC AAC
8	NLRP3 Δ8 product A	AAA AGA TCT CTC AGC AAA TCA GGC TGG AG	AAA CAG ACA ACT CCA ACA CCT GAA GCT
9	NLRP3Δ8 product B	AAA TCT AGA CTA GTC ATC TAC TCG AG	AAA GTG TTG GAG TTG TCT GAA ATG TAT
10	NLRP3 Δ9 product A	AAA AGA TCT CTC AGC AAA TCA GGC TGG AG	AAA TAC TCG AGC TAC CCA GGT TCT GCA GGA
11	NLRP3 Δ9 product B	AAA TCT AGA CTA GTC ATC TAC TCG AG	AAA AAC CTG GGT AGC TCG AGT AGA TGA
12	NLRP3	AAA AGA TCT CTC AGC AAA TCA GGC TGG AG	AAA TCT AGA CTA GTC ATC TAC TCG AG
13	NLRP3 LRR-only FL, Δ5, Δ6, Δ7, Δ8	AAA GGA TCC ATG TAT ACA GAC ATA GAG ATG AAC CGA CTT GGA AAG GGA TTG GTG AAC AGC CAC CTC ACT T	AAA GGA TCC ATG TAT ACA GAC ATA GAG ATG AAC CGA CTT GGA AAG GGA TTG GTG AAC AGC CAC CTC ACT T
14	NLRP3 LRR-only Δ4	AAA GGA TCC ATG TAT ACA GAC ATA GAG ATG AAC CGA CTT GGA AAG GGA TTG GGG CGC TGT GGC CTC TCG	TTT TCT AGA CTA CCA AGA AGG CTC AAA GAC
15	NLRP3 LRR-only Δ9	AAA GGA TCC ATG TAT ACA GAC ATA GAG ATG AAC CGA CTT GGA AAG GGA TTG GTG AAC AGC CAC CTC ACT T	TTT TCT AGA CTA CCC CAG GTT CTG CAG GAG GCA GC
16	NLRP3 NACHT-only	AAA GGA TCC ATG GAT TAC AAG GAT GAC GAC GAT AAG GAT TAC CGT AAG AAG TAC AGA A	TTT TCT AGA TTA TCC ATG AGA ACA GGC AGC ATG A
17	NLRP3 R262W	ACT ATC TGT TCT ATA TCC ACT GTT GGG AGG TGA GCC	ACT ATC TGT TCT ATA TCC ACT GTT GGG AGG TGA GCC
18	NLRP3 L305P	CAA AGG CAC CTT GCG GCT CAT CGA AGC CG	CGG CTT CGA TGA GCC GCA AGG TGC CTT TG
19	NLRP3 L353P	GCT GCA GTT TCT CCG GGG CCA CAG GTC TC	GAG ACC TGT GGC CCC GGA GAA ACT GCA GC
20	NLRP3 E567K	AAA AAT CAA ATA CCC CTT TTT GAA TTT GCC ATA GTT TTC CAG AAG GA	TCC TTC TGG AAA ACT ATG GCA AAT TCA AAA AGG GGT ATT TGA TTT TT
21	sg-NLRP3	CAC CGA TCG CAG CGA AGA TCC ACA	AAA CTG TGG ATC TTC GCT GCG ATC
22	sg-Luciferase	CAC CGC TTC GAA ATG TCC GTT CGG T	AAA CAC CGA ACG GAC ATT TCG AAG C